

This article was downloaded by:[NEICON Consortium]
[NEICON Consortium]

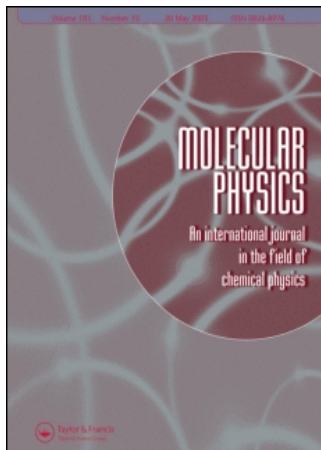
On: 26 January 2007

Access Details: [subscription number 762905488]

Publisher: Taylor & Francis

Informa Ltd Registered in England and Wales Registered Number: 1072954

Registered office: Mortimer House, 37-41 Mortimer Street, London W1T 3JH, UK



Molecular Physics

An International Journal in the Field of Chemical Physics

Publication details, including instructions for authors and subscription information:

<http://www.informaworld.com/smpp/title-content=t713395160>

Theoretical estimate of ortho-para separation coefficients for H₂ and D₂ on A-type zeolites for small and medium coverage

Alexander V. Larin^a; Victor S. Parbuzin^a

^a Department of Chemistry, Moscow State University, Leninskie Gory, Moscow, B-234, GSP 119899, Russia

To link to this article: DOI: 10.1080/00268979200102841

URL: <http://dx.doi.org/10.1080/00268979200102841>

Full terms and conditions of use: <http://www.informaworld.com/terms-and-conditions-of-access.pdf>

This article maybe used for research, teaching and private study purposes. Any substantial or systematic reproduction, re-distribution, re-selling, loan or sub-licensing, systematic supply or distribution in any form to anyone is expressly forbidden.

The publisher does not give any warranty express or implied or make any representation that the contents will be complete or accurate or up to date. The accuracy of any instructions, formulae and drug doses should be independently verified with primary sources. The publisher shall not be liable for any loss, actions, claims, proceedings, demand or costs or damages whatsoever or howsoever caused arising directly or indirectly in connection with or arising out of the use of this material.

© Taylor and Francis 2007

Theoretical estimate of *ortho*–*para* separation coefficients for H₂ and D₂ on A-type zeolites for small and medium coverage

By ALEXANDER V. LARIN and VICTOR S. PARBUZIN

Department of Chemistry, Moscow State University, Leninskie Gory, Moscow
B-234, GSP 119899, Russia

(Received 25 April 1992; accepted 6 May 1992)

Ortho–*para* separation coefficients for H₂ and D₂ are estimated for small and medium coverage of 4A and 5A zeolites using the assumption that two types of adsorption sites occur. Charge distribution of zeolite ions is modelled by fitting theoretical to experimental band shifts of physisorbed diatomic molecules of hydrogen, deuterium and nitrogen. Computed and experimental values of *ortho*–*para* separation coefficients for H₂ and small coverage of 4A zeolite have been demonstrated to agree reasonably well. The reasons for the discrepancy between the theoretical and experimental *ortho*–*para* separation coefficients for higher coverage are discussed.

1. Introduction

Zeolites are widely used on laboratory and industrial scales for the separation of gas mixtures, e.g. for the separation of isotopic and spin modifications of dihydrogen [1–7]. Abundant experimental data have been thus far collected in this field. However, the theoretical treatments of these data are not numerous [8, 9], and here are undertaken for a model with homogeneous zeolite ‘surface’. It is clear that more realistic microscopic interpretation of the adsorbed state can be achieved primarily for a relatively simple and well studied adsorbent such as zeolite A and model adsorbates for which quantitative data on polarizabilities, multipole moments and molecular geometry are available. As a rule, for the systems under discussion, viz. modifications of molecular hydrogen adsorbed on A-type zeolites, adsorption parameters (e.g., heat of adsorption, separation coefficients) are highly dependent on coverage that is indicative either of considerable energetic inhomogeneity of adsorbent surface (different types of adsorption centres occur), or of marked adsorbate–adsorbate intermolecular interaction. The latter factor is negligible for small coverage. Since the experimental data on medium and high coverage are a poor source of information on the relative contributions of heterogeneity and intermolecular interactions, the only way to get such information is by theoretical computations. This approach necessarily involves the computation of zeolite–adsorbate interaction energy (IE).

Such approaches to the calculation of the IE of atoms and polyatomic molecules with zeolites are hindered by the lack of reliable data on parameters (polarizabilities $\alpha(Z)$, charges $q(Z)$, van der Waals radii $r(z)$) of adsorbent ions ($Z = \text{Na, Ca, Si, Al, O}$). We have proposed a new method for their estimation based on the use of another source of experimental data, namely band shifts ($\Delta\nu$) of the physisorbed diatomic molecules H₂, D₂, and N₂ [11–13]. A consistent description of experimental shifts

Δv for H_2 , D_2 , and N_2 [14–16] has been obtained using a unique set of zeolite ion parameters ($\alpha(Z)$, $q(Z)$, $r(Z)$). Consideration of the interaction energy surface for the system $H_2(D_2)$ –zeolite A reconstructed with this set of parameters allowed us to make use of the lattice theory of adsorption with two kinds of adsorption sites. This model is applied in the present work to the calculation of *ortho-para* (*o-p*) separation coefficients for H_2 and D_2 for small and medium coverage of zeolite surface. Theoretical estimates are then compared with experimental data. Applications of this model to the calculation of H_2 , D_2 isotherms and isotopic separation coefficients for H_2/D_2 will be presented elsewhere.

2. Calculation of adsorbate–zeolite interaction energy

Details of the computation technique is given in reference [13]. Here we present a brief account of the steps of the IE calculation. Previous information on the characteristics of the interacting components, zeolite and adsorbate molecule, will be given below.

Zeolites 4A and 5A are considered as sets of ions with coordinates fixed in agreement with the spatial symmetry group Fm3c (see table 1) [17]. As to zeolite 5A, the coordinates of sodium and calcium ions were taken from x-ray data treated with the Pm3m group approximation [18] and the positions of other ions were taken as for zeolite 4A, due to the small difference between the ion's positions in both forms. The internal 'surface' of the unit cell (UC) available for our adsorbate is formed by "rings" of Si, Al, and O atoms. The rings are named 4-, 6-, 8-rings in accordance with the number of Si and Al atoms in the ring, and are located in the direction of two-, three- and fourfold symmetry axes. The spherical coordinates of the axes are shown in figure 1. The cations Na_{III}^+ , Na_I^+ , Na_{II}^+ reside approximately in the centres of the corresponding rings. The preference for the model responding to the Na_{III}^+ location in one of the 12 degenerate positions was determined in accordance with the relation of the adsorption times of the molecule at the adsorption centre and of the sodium at a degenerate position. The adsorption time was estimated qualitatively provided that the most weakly coordinated Na_{III}^+ might be considered as an "adsorbed" ion. In accordance with Frenkel's expression, the adsorption time $\tau = \tau_0 e^{Q/RT}$ [19], where τ_0 is the period of vibration in a direction perpendicular to a surface and Q is the heat of adsorption on the homogeneous surface or, for the case

Table 1. Coordinates (Au) of the ions of zeolite 4A [17] (1 Au = 0.52917 Å).

Ion	X	Y	Z
Na _I	-6.9786	-6.9786	-6.9786
Na _{II}	-1.8045	-1.5544	-11.6001
Na _{III}	-6.6816	-6.6816	0.0000
O _I	-11.6001	-5.2743	-0.1564
O _{II}	-11.6001	-4.8911	-4.8298
O _{III}	-9.1042	-8.8787	-3.6415
Si	-11.6001	-7.2774	-3.0165
Al	-11.6001	-2.9163	-7.4045
Na ^a	-7.9837	-7.9837	-7.9837
Ca ^a	-7.1028	7.1028	7.1028

^a For zeolite 5A [18].

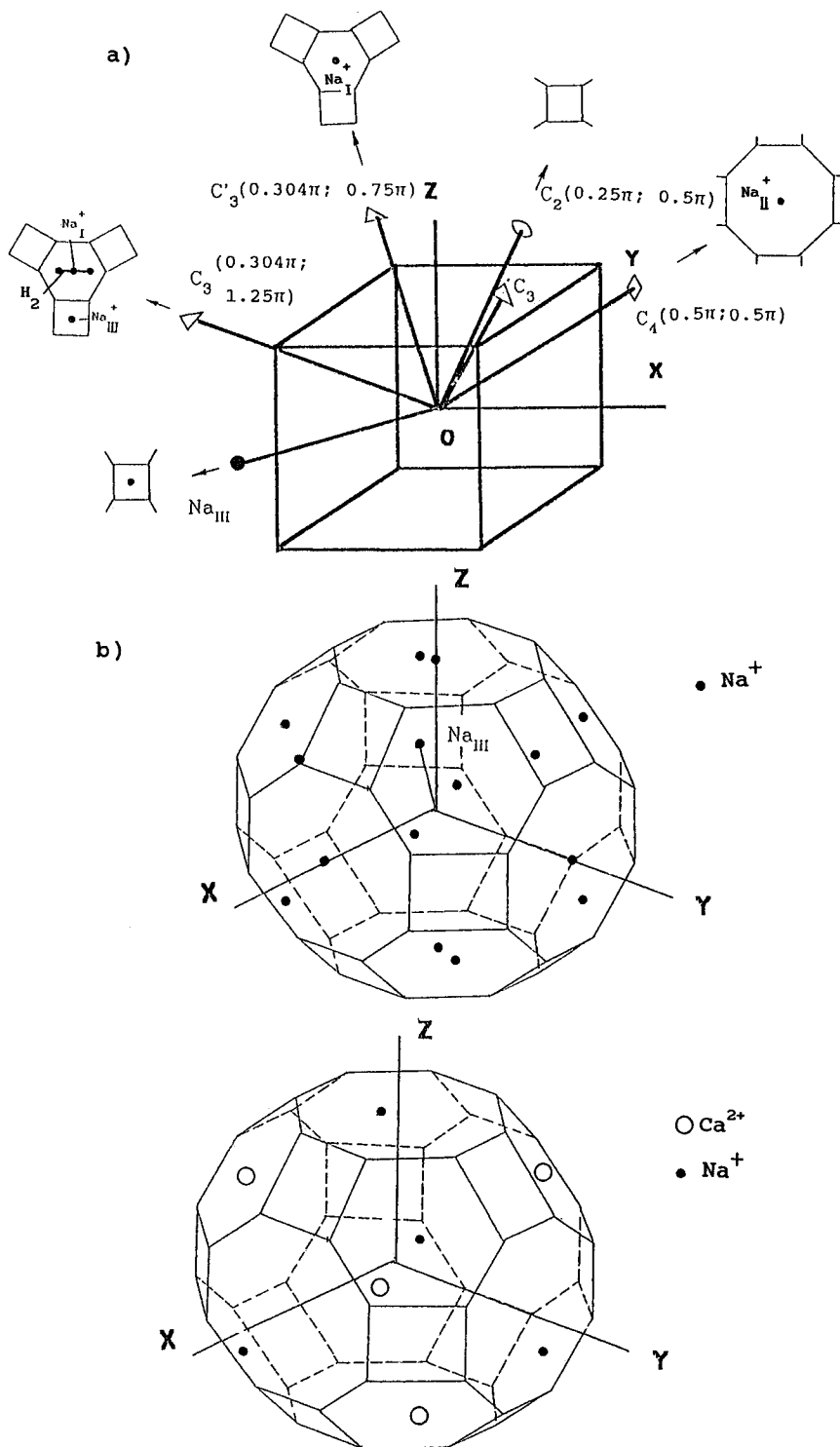


Figure 1. The coordinate system (a) is related with the centres of the cells of the zeolites 4A (b) and 5A (c). The position of the Na_{III}^+ cation and some axes (a) are shown (spherical coordinates are given in brackets) for zeolite 4A. Corresponding rings (a) are presented in the directions of the symmetry axes. The corners of the cube in (a) correspond to Na^+ (for zeolite 4A), and to Na^+ , Ca^{2+} (for zeolite 5A) positions.

of Na_{III}^+ , the barrier value between the degenerate positions (the whichever has the greater heat of adsorption). The wavenumber values of the Na^+ vibration frequency corresponding to the period τ_0 in zeolite 4A were determined to be near 200 cm^{-1} [20], and are of the same order as the wavenumber values of radial vibration (corresponding to period τ'_0) calculated by us for molecular hydrogen from 90 cm^{-1} to 219 cm^{-1} . So the approximate equality $\tau_0 \cong \tau'_0$ was proposed. The value of Q for the lower coordinated ion Na_{III}^+ was connected with the activation energy of the electric conduction of dehydrated zeolite 4A (59 kJ mol^{-1}) [21], while the adsorption energy Q of hydrogen is equal to 8.8 kJ mol^{-1} [3]. Then a qualitative estimation made in accordance with the Frenkel proportionality shows that the adsorption time of Na_{III}^+ is essentially greater than the analogous adsorption time of the adsorbate molecule for the temperature range $50\text{--}200 \text{ K}$ ($\tau/\tau' \cong e^{(Q-Q')/RT}$ range is $10^{52} - 10^{13}$). It allows us to consider a single Na_{III}^+ per UC. In spite of the introduction of a single ion Na_{III}^+ into UC of zeolite 4A, we use the conventional notation for the axes as C_3 , C_2 , C_4 .

Molecular sizes and molecular constants are presented in Table 2. According to estimates [3], the saturation of zeolite 4A corresponds to 14–16 molecules per UC.

Taking into account the electrostatic E_{el} , inductive E_{ind} , dispersive E_{disp} , repulsive E_{rep} , and intermolecular E_{im} components, the total IE (E_{tot}) was calculated as

$$E_{\text{tot}} = E_{\text{el}} + E_{\text{ind}} + E_{\text{disp}} + E_{\text{rep}} + E_{\text{im}}, \quad (1)$$

where representation of the components are briefly given in the appendix. The E_{im} was calculated using the interaction between the molecules from the same UC only. The near spherical shape of cages of zeolite type A with the small "windows" (8-rings) between the cages mean that we can consider adsorbate molecules in the same cage as isolated with respect to any interaction with the adsorbate molecules in the nearest cages. Values of E_{im} (denoted as w_1 , w_2) and total IE are given in figure 2. (The latter relation (E_{tot} and w_1 , w_2) does not change essentially with replacing expression (A12) by the Kihara potential, so we did not discuss the small effects related to the choice of the molecular shape (spherocylinder of ellipsoid) due to the small contributions of the intermolecular repulsion dependent on this choice.) The comparison of the total IE components in different directions is presented in the figure 3 for the most energetically profitable orientation of the molecular axis (the lowest curves in figure 4).

In order to define possible adsorption sites (AS) we have computed IE for a large number of molecular orientations relative to the axes between the centre of the lattice fragment (one of the rings) and UC centre (three of the orientations are shown in the

Table 2. Constants of the adsorbate molecules H_2 , D_2 , N_2 (Au)^a

Gas	$r_{\parallel}/\text{\AA}^b$	$r_{\perp}/\text{\AA}$	r_0	θ_{zz}	Φ_{zzzz}	α_{\parallel}	α_{\perp}
H_2	1.95	1.54	1.446	0.967	0.42	6.763	4.739
D_2	1.95	1.54	1.437	0.952	0.42	6.651	4.692
N_2	2.00	1.60	2.006	-0.989	-7.50	15.036	9.662

^a $1 \text{ kJ mol}^{-1} = 3.806 \times 10^{-4} \text{ Au}$; $1 \text{ m} = 1.889 \times 10^{10} \text{ Au}$; $1 \text{ C} = 6.241 \times 10^{18} \text{ Au}$ of charge.

^b Molecular models correspond to spherocylinders with volume $(4/3)\pi r_m^3$ and axes relation $r_{\parallel} = r_{\perp} + \frac{1}{2}r_0$ [10], where $r_m = 3.49 \text{ \AA}$ for H_2 , D_2 [41] and $r_m = 3.76 \text{ \AA}$ for N_2 [42].

^c References [31–35].

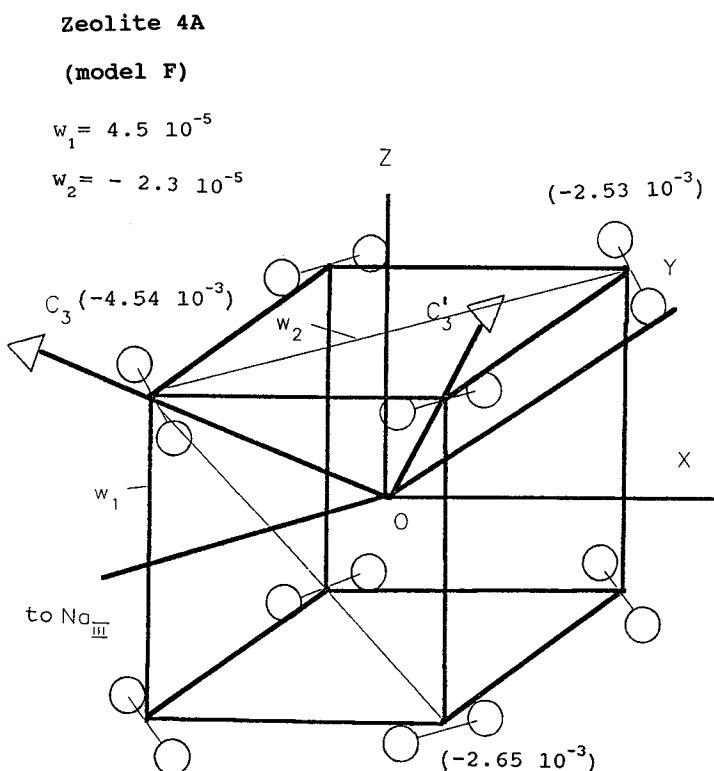


Figure 2. Intermolecular interaction energies w_1 , w_2 (Au) between molecules adsorbed on neighbouring sites. Values of IE (Au) for the different sites are shown in brackets.

figure 4). The results of computation of the IE of H_2 at the radial coordinate with orientation of molecular axis corresponding to the IE minimum (see figure 5) reveal that the two deepest wells occur at those C_3 axes closest to the Na_{III}^+ ion. Both these points (1st type of AS) are the most probable adsorption centres at the temperature of spectroscopic measurement (90 K [15]), and thus the values Δv were determined for AS of the first type (see molecular position in figure 1).

3. Calculation of band shift values and zeolite models

The shift of a frequency of the internuclear vibrational transition $v-v'$ band may be expressed by relation (2) (see figure 6)

$$\Delta v = \langle v' | V^{(v')} | v' \rangle - \langle v | V^{(v)} | v \rangle + \Delta v_{\theta, \phi} + \Delta v_R \quad (2)$$

where an accurate presentation $V^{(v)}$ of the operator of the IE in the v vibrational state will be given below (see equation (3)), but the average value $V^{(v)}$ may be estimated roughly as E_{tot} with some corrections depending on an average amplitude of vibration; small contributions come from the differences in the energy levels of a hindered rotator ($\Delta v_{\theta, \phi}$) and of molecular centre of gravity motions (Δv_R) in the upper and lower states of the internuclear vibrational transition $v - v'$. The E_{im} was not calculated in the estimation of the band shift, taking into account the low coverage due to appropriate experimental conditions (0.5 molecule per UC) [14].

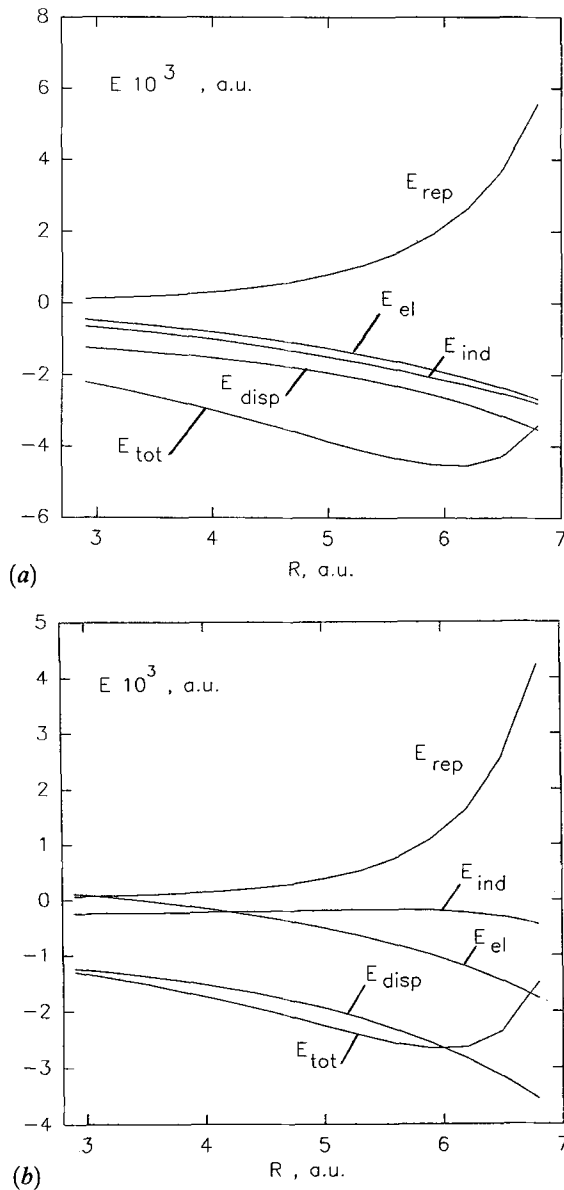


Figure 3. Interaction energy (IE) components for the most energetically favourable position of the molecular axis of H₂ with zeolite 4A along the C₃ (a) and C_{3'} (b) axes. The components are labelled as follows: el, electrostatic; ind, inductive; disp, dispersive; rep, repulsive; tot, total energy.

The components of the IE depend on the large number of zeolite parameters ($\alpha(Z)$, $q(Z)$, $r(Z)$, $Z = \text{Na, Ca, Si, Al, O}$) for the band shift data to be fitted to experiment without some additional restrictions on the parameters. For convenience we shall use the ionicity [24] $q_0 = q(\text{Na}) + q(\text{Si}) + q(\text{Al}) = |q(\text{O}_I) + q(\text{O}_{II}) + 2q(\text{O}_{III})|$ as characteristic of the total charge of the cationic or anionic framework on the zeolite. The ionicity can vary in the range $0 < q_0 < 8$. For further simplification we propose the following four assumptions about the zeolite parameters. 1. The sodium

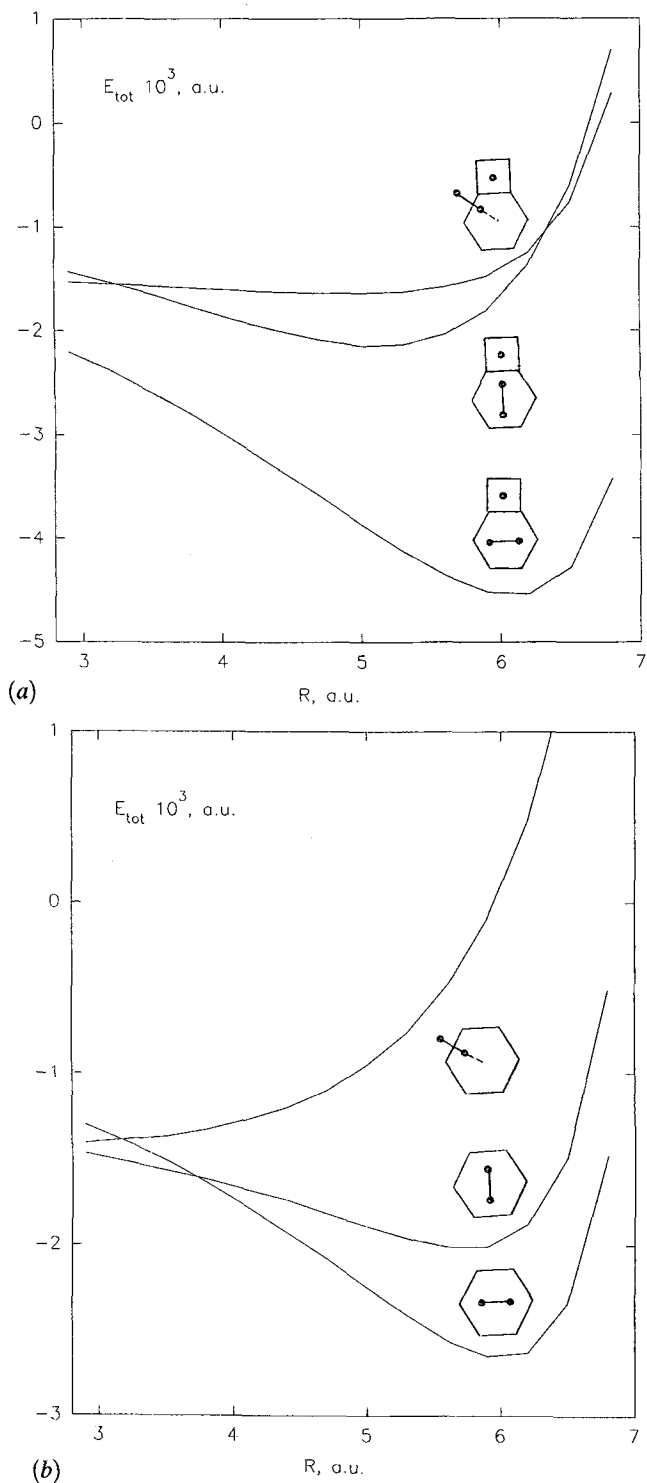


Figure 4. Total interaction energy (IE) for H_2 with zeolite 4A for different positions of the molecular axis along the C_3 (a) and C_3' (b) axes. The positions of the molecular axis are shown.

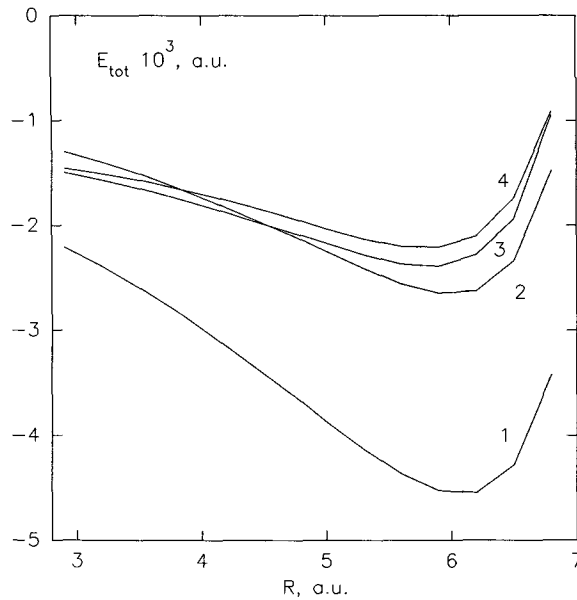


Figure 5. Total interaction energy (IE) for the most energetically favourable position of the molecular axis of H_2 with zeolite 4A along different axes. The coordinates (θ, Φ) of the symmetry axes are as follows: 1, $C_3 (0.304\pi; \frac{5}{4}\pi)$; 2, $C'_3 (0.304\pi; \frac{7}{4}\pi)$; 3, $C_4 (\frac{1}{2}\pi; \frac{1}{2}\pi)$; 4, $C_2 (\frac{1}{4}\pi; \frac{1}{2}\pi)$.

ions of different crystallographic types (Na_I, Na_{II}, Na_{III}) have equal charges (+1). 2. The oxygen ions of different crystallographic types (O_I, O_{II}, O_{III}) have equal charges. 3. The van der Waals radius of an ion is a continuous function of an ion's charge. We assume a linear dependence for all ions (see table 3) using data [25–27] for the

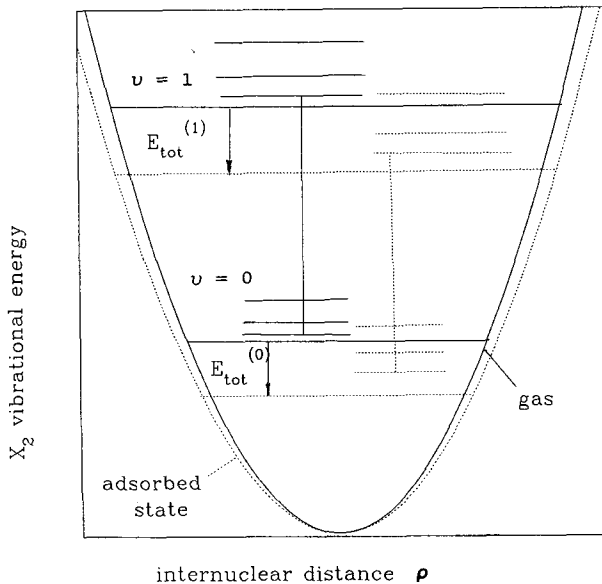


Figure 6. Band shift for a vibrational transition.

Table 3. Parameters of van der Waals radius dependence of the ion Z ($r(Z^q) = aq(Z) + b$).

Z	$b/\text{\AA}$	$a/\text{\AA Au}^{-1}$
Na	1.54 ^a	1.058
O	1.15	0.290 ^b
Si	1.18 ^c	0.383
Al	1.11 ^c	0.554
Ca	1.97 ^a	0.300

^a Values of a and b are estimated according to reference [25].

^b Value is obtained taking into account $R(\text{O}^0) = 1.52$ [28], $R(\text{O}^{2-}) = 2.10 \text{\AA}$ [43].

^c Values of a and b are estimated according reference [26].

constants of this dependence to be defined. We must note that only the dependence of the van der Waals radius of oxygen has a real significance for the IE calculation. The dependence of Si and Al ions has a rather symbolic sense owing to the small contributions of the repulsive component of IE [13]. The dependence of the sodium ion is not valid due to assumption 1 (except the single case considered below with $q(\text{Na}) = 0.9$). 4. The polarizability of an ion is a continuous function of an ion's charge. A linear function for the polarizability of the oxygen ion was suggested, and used by Kiselev *et al.* [28]. From the results of *ab initio* calculations [30] we extracted the exponential dependence for Si and Al ions (see table 4), and linear for Na (see table 5). The exponential form is not the only one possible. However, the error in the IE resulting from using a parabolic function through the calculated points is not more than 1–2%. Such an error is permissible for the calculation of band shift values less than 10% of the IE for H_2 adsorbed on zeolite 4A. Allowance for the polarizability dependence for Si and Al ions corrects essentially the value of the calculated IE so that the error is about 30% (for the zeolite model with ionic charges of Si, Al to be 0.7–0.8) in a case where one disregards the contributions of dispersive interactions between Si or Al ions and molecules [13]. The dependence of the sodium ion is not valid due to assumption 1 (except the single case considered below with $q(\text{Na}) = 0.9$).

On the basis of assumptions 3 and 4, it is possible to decrease the number of unknown parameters to the number of the charges $q(Z)$. So, considering assumptions 1 and 2, the unknown charges are connected by the relation $q_0 = 1 + q(\text{Si}) + q(\text{Al}) = 4|q(\text{O})|$. As we found, the difference between the Si and Al charges (and, as a result, the difference between the polarizabilities) has an insignificant influence on the IE and the calculated band shift [13]. Consequently, $q(\text{Al})/q(\text{Si})$ was taken as constant (0.975) for like compounds [29]. Then the ionicity

Table 4. The parameters A, B, C of the dependence of the polarizabilities of Si and Al on the charge q ($\alpha(Z) = A \exp(-(q(Z) - B)^2/C)$).

Z	A	B	C	Polarizability ^a /Au ³		
				$q = 0$	$q = 1$	$q = 2$
Si	0.109	-10.70	-19.40	39.61	13.84	5.36
Al	0.013	-12.39	-19.13	38.29	11.05	3.54

^a α was calculated in accordance with results noted in reference [30] via formula (A6).

Table 5. The parameters A , B of the dependence of the polarizabilities of Na and O on the charge $q(\alpha(Z) = A - Bq(Z))$.

Z	$B/\text{Au}^3 \text{ \AA}^{-1}$	Polarizability ^a α/Au^3		
		$q = 0$ (A)	$ q = 1$	$ q = 2$
Na ^a	27.94	29.78	1.83	—
O ^b	9.38	7.55	16.93	26.31

^a Estimated according to reference [30].^b From reference [28].

becomes proportional to the unknown charges: $q_0 = 1 + 1.975q(\text{Si}) = 4|q(\text{O})|$. By fitting the single parameter, the ionicity, to decrease the difference between the computed and experimental band shifts for physisorbed diatomic molecules, we were able to model some characteristics of zeolite 4A (see table 6). The additional difficulty due to unknown calcium ion charge in the case of zeolite 5A was solved by the proposition about the equality of the ionicities of the 4A and 5A forms. To estimate the calcium ion charge we fix the q_0 of zeolite 5A and vary $q(\text{Ca})$ until the agreement is achieved between the calculated $\Delta\nu$ and experiment. Realizing the fact that some parameters ($r(\text{O}^0)$, $q(\text{Na})$, $q(\text{O}_I)/q(\text{O}_{II})$, $q(\text{O}_{III})/q(\text{O}_{II})$, where $r(\text{O}^0)$ is the van der Waals radius of the oxygen atom) have not been proved by self-directing estimations, we calculate the zeolite models with the variation of these parameters. The best model F (further used for determination of the free volume v_f^1 and adsorption energy ϵ_1) meets the requirement for the nonintersection of the spheres of oxygen ions ($r(\text{O}^{-0.725}) = 1.36 \text{ \AA}$) contained in the same tetrahedron SiO_4 (AlO_4). The bounds of the spheres may be calculated easily (1.29–1.40 \AA) from the distances Si—O, Al—O, which are 1.597 and 1.731 \AA [17], respectively. The change of oxygen radius $r(\text{O}^q)$ with the charge q (for different models) is not large, so that the radius lies in the customary region 1.3–1.6 \AA for all zeolite models (except model H). The problem of the choice of zeolite characteristics is sophisticated enough and the unique model cannot be defined. We have considered here a set of models

Table 6. The zeolite 4A^a models giving agreement of calculated and experimental shifts ($q(\text{Na}) = 1.0$; $q(\text{Al})/q(\text{Si}) = 0.975$).

Model	q_0/Au^b	$\frac{q(\text{O}_I)}{q(\text{O}_{II})}$	$\frac{q(\text{O}_I)}{q(\text{O}_{II})}$	$r(\text{O}^0)/\text{\AA}$
A ^c	1.2	1.00	1.00	1.15
B	1.7	0.50	1.00	1.15
C	1.8	1.00	1.00	1.45
D	2.1	1.00	1.00	1.35
E	2.4	0.75	1.25	1.15
F	2.9	1.00	1.00	1.15
G	3.5	1.00	1.00	1.05
H	6.8	1.00	1.00	0.65

^a Ionic characteristics of zeolite 5A are obtained for model F with $q(\text{Na}) = 1.0$; $q(\text{Ca}) = 1.5$.^b $q_0 = q(\text{Na}) + q(\text{Si}) + q(\text{Al}) = |q(\text{O}_I) + q(\text{O}_{II}) + 2q(\text{O}_{III})|$.^c $q(\text{Na}) = 0.9$.

(A–H) chosen to reproduce the main tendencies in the variation of the zeolite parameters.

For all the models that we considered, the IE minima for AS of the 1st type were the deepest. Next to them were the potential wells at C'_3 axes (2nd type of AS) and at C_4 . The differences in the IE of the AS originate in the position of an AS relative to a Na_{III}^+ ion. The increased components E_{ind} , E_{el} on the 1st type AS are due mainly to the higher field and field gradient in the corresponding position C_3 (see figure 3).

The introduction of a single ion Na_{III}^+ into the UC of zeolite 4A necessitates the introduction of some variants in the arrangement of the Na_{III}^+ ions in surrounding UC's. The calculations show the only changes in the relative IE values of a molecule located on an AS of the 2nd type and the other AS having comparatively low IE in relation to the IE of a molecule located in the "deepest" minima [20]. Here we do not discuss the probable models with another choice of AS of the 2nd type (see section 7). Intermolecular interaction energies have been computed for the most energetically favourable orientations at AS of the 1st and 2nd kinds (see figure 2), and then used for calculations of lattice partition functions and thermodynamic values.

4. Models of adsorbed molecules

Correct choice of model of the adsorbed molecule has both thermodynamic and spectroscopic aspects. This work is devoted to the calculation of thermodynamic values which requires thorough choice of the relevant models. Such a tight interrelation between the choice of the model and the predicted thermodynamic values is a consequence of quantum nature of adsorbed hydrogen molecules, estimations of the partition functions and exclusion from the adsorption energy of the zeroth energies of the hindered rotation and motions of the gravity centre of the molecule (see equation (8)). The contributions of the shifts of hindered rotation levels or levels corresponding to motions of the centre of gravity of the molecule are small enough with respect to the total value Δv [11].

Six degrees of freedom—translations (R, θ, Φ), rotations (ϑ, ϕ), and intramolecular vibration (ρ) (see figure 7)—were involved in modelling of the motion of diatomic molecule near a set of fixed zeolite ions. The approximations used therein are described below.

4.1. Models of translational and vibrational motions of adsorbed molecules

Intramolecular vibrations of adsorbed molecules are treated in terms of a perturbed harmonic oscillator. The zeroth approximation corresponds in our case to a harmonic oscillator (HO) in the gas phase and for different vibrational levels parabolaes with coordinates ρ_v were used. The interaction energy operator was then introduced (perturbation) and represented as the following truncated expansion

$$V^{(v)} = \sum_{n=0}^{n_e} \frac{k_n^{(v)}}{n!} x_v^n, \quad (3)$$

where $x_v = \rho - \rho_v$; $k_n^{(v)}$ are coefficients of expansion over the powers of ρ_v ; v is the quantum number of the intramolecular vibration of an adsorbate; $(n_e + 1)$ is the number of members in the expansion. Average internuclear separations ρ_v , polarizabilities, and multipole moments for different vibration states (0, 1, 2) were chosen in accordance with the results of references [31–35] (see table 2). Detailed comments on the computation of such series can be found in reference [12].

In the adsorbed state, translational motions of the free molecule transfer into one vibration of the centre of gravity of the molecule over radial coordinate R , and two hindered motions over angular coordinates θ, Φ .

Radial motion of the centre of gravity was described using the HO approximation. Vibrational frequencies $w_R^{(I)}$ (for AS of the I type, $I = 1, 2$) of isotopic modifications were chosen by fitting them to values giving reasonable agreement between calculated and experimental isotopic separation coefficients for small and medium coverage [22].

As to the angular θ, Φ motions of the centre of gravity, the corresponding partition function may be treated classically, at least within the temperature range of interest. We have already established that the IE wells along the chosen directions (C_2, C_3, C_4) differ in depth, while the radial coordinate of the minima remains almost the same for all axes (see figure 5). The latter trend allows the use of the hindered rotator approximation, in which an adsorbate molecule and zeolite crystal are taken as a whole with the mass concentrated at the centre of the UC, with the rotation constant $B_{Z-H_2} = 1/(2m_{H_2}R_{H_2}^2) = 7.3 \times 10^{-6}$ Au, where R_{H_2} is radial coordinate of molecular centre.

Since B_{Z-H_2} is small compared with the structure of the vibrational energy states normal both to the plane of the ring ($hcw_R^{(I)} \cong 10^{-3} - 4 \times 10^{-4}$ Au, for As of the I th type) and to the rotation coordinate (rotational constant $B_{H_2} = 2.89 \times 10^{-4}$ Au), the partition function for angular motion may be separated from these motions. Since B_{Z-H_2} is small compared with kT ($kT = 1.6 \times 10^{-4} - 4.7 \times 10^{-4}$ Au for temperatures of 50–160 K) this partition function may be treated classically. The corresponding quantum corrections to IE [10] turned out to be small and were estimated using analytical formulae with the assumption that the profiles of the IE by coordinates θ, Φ can be described locally as $U_\theta P_2^0(\theta)$ and $U_\Phi \sin(4\Phi)$, where $P_2^0(\theta)$ is a Legendre polynomial; and U_θ, U_Φ are coefficients produced by numerical approximation of the IE surface along the corresponding coordinate without fitting [22].

4.2. Model of rotational motion of adsorbed molecule

To describe the hindered rotation we have used the Evett–Sams–MacRury potential [36, 37] in the form

$$V(\vartheta, \phi) = \lambda \cos^2 \vartheta + \mu(1 - \cos(n\phi)), \quad (4)$$

where coordinate ϑ corresponds to the rotation of the molecular axis in a plane defined by the molecular axis and the radius-vector of the molecular centre of gravity originating at the centre of the UC, and coordinate ϕ is the rotation in a plane normal to the radius vector and intersecting it at molecular centre of gravity (see figure 7; $n = 2, 3$; λ, μ are produced from numerical approximation of the IE surface along coordinates ϑ, ϕ and expressed in units of the rotational constant B_X . Otherwise, ϕ and ϑ rotations might be viewed alternatively as rotations in the planes one of which is parallel and the other perpendicular to the corresponding ring plane.

Eigenvalues $\epsilon_{k|p,q}$ of the Hamiltonian (5) including the potential from equation (4)

$$\left\{ \frac{1}{\sin \vartheta} \frac{\partial}{\partial \vartheta} \left(\sin \vartheta \frac{\partial}{\partial \vartheta} \right) + \frac{1}{\sin \vartheta} \frac{\partial^2}{\partial \phi^2} + V(\vartheta, \phi) - \epsilon_{k|p,q} \right\} F_{k|p,q}(\vartheta, \phi) = 0 \quad (5)$$

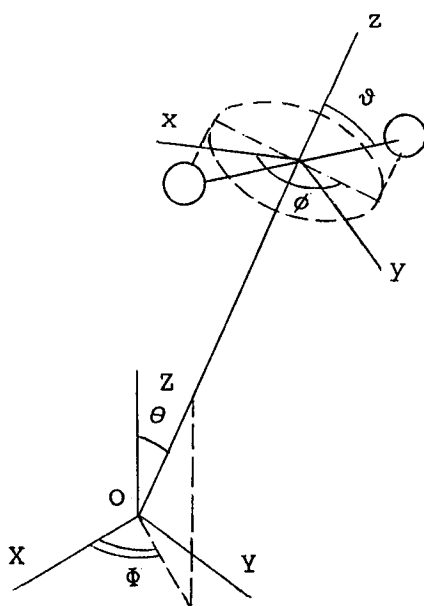


Figure 7. The coordinate system for a diatomic molecule.

where $F_{k|p,q}(\vartheta, \phi)$ is the rotational function, were found by a variational procedure based on a published approach [37] and implemented as a computer program.

All models (see table 6) of A-type zeolites under consideration have an important common feature to reveal several kinds of adsorption centres with different values of λ and μ and, as a consequence, different structures of rotation states (see table 7). The data of table 8 show that in the deepest well of the IE surface of H_2 (at the C_3 axis near the Na_{III}^+ ion) the variation in the rotation barrier μ is due mainly to the differences in the interaction energy of the adsorbate with the Na_{III}^+ ion, resulting in lowering of the symmetry of the potential down to $n = 2$. Expression (4) with $n = 3$ turned out to be the most suitable for approximating the H_2 on zeolite 5A

Table 7. The parameters λ and μ of potential (2) for hydrogen on the different adsorption sites of zeolites 4A^a, 5A^b.

$\frac{\theta}{\pi}; \frac{\phi}{\pi}$	$\frac{-E_{tot}^d 10^3}{Au}$	$\frac{\lambda^e}{B}$	$\frac{\mu^e}{B}$	$\frac{\epsilon_{ 1,1\rangle}}{Au}$
Zeolite 4A				
0.304; 1.25	4.540	11.20	5.66	1.625
0.304; 1.75	2.653	10.48	1.29	0.976
0.500; 0.50	2.787	7.07	3.59	1.201
Zeolite 5A				
0.304; 1.75	5.142	22.00	0.00	1.080
0.304; 1.25	2.439	10.70	0.00	0.377

^a Three directions correspond to the sites of 1st, 2nd type, and axis C_4 (see text, section 2).

^b Two directions correspond the axes C_3 directed on $Ca^{+1.5}$ (site of 1st type), Na^{+1} (2nd type).

^c Spherical coordinates θ, ϕ of the adsorption sites are shown in figure 1.

^d E_{tot} is the total interaction energy.

^e Rotational constant $B = 2.89 \times 10^{-4} Au$.

Table 8. The dependence of the parameters λ and μ of the potential $\lambda \cos^2 \vartheta + \mu(1 - \cos(n\phi))$ on the number of ions of zeolite 4A to be taken into account.

Number of ions ^a (Na _{III} ions)	Unit cell number	λ/B	μ/B
134(0)	1	9.39	0.696
135(1)	1	10.94	5.743
141(7)	1	10.65	5.625
309(7)	1	10.80	5.631
1563(7)	7	11.13	5.634
2727(27)	27	10.07	5.640

^a The number of ions related to the central UC varies because of the inclusion of some ions from the nearest UC's.

interaction energy surface, but small values of μ let us neglect perturbation due to ϕ rotation and thus to simplify the solution.

Lowering of symmetry of the IE surface due to the Na_{III}⁺ ion might lead to different coordinates ϑ, ϕ for the centres of different types, and we have checked this. For both the 1st and 2nd types of AS, the minimal energy of rotation was found to correspond to rotational momentum quantization along the axis passing through the molecular centre of gravity and the ion Na_I⁺.

Convergence of IE values has been demonstrated previously [38] to be achieved if ions of not less than seven elementary cells of zeolite were involved. On the other hand, the convergence of the factors λ, μ of the model potential expressed as in equation (4) over coordinates λ, μ is achieved if ions of one cell are involved in computations. Convergence of the values of λ and μ with the variation of the number of ions involved in the computation of interaction energy (see table 8) reveals the convergence of the gradient of the field. The latter as we have elucidated is the main contribution to rotation barriers λ and μ .

5. Method of calculation of the adsorption isotherm and σ - p separation coefficients of isotopic modifications of molecular hydrogen

Calculation of thermodynamic parameters as functions of coverage requires knowledge of the grand partition function [39]. To evaluate it, we have introduced the following seven simplifying assumptions.

- 1, Zeolite parameters are independent of coverage.
- 2, Adsorption sites are located at the vertices of a cube (analytical expressions for the lattice partition function for eight regularly assembled adsorption sites can be found in tables 9 and 10).
- 3, Adsorption occurs over an inhomogeneous surface of zeolite UC, on which the sites of two kinds from 2 and 6 centres for zeolite 4A (from 4 and 4 centres for 5A) differ in adsorption energy ϵ_1 and free volume v_f^1 (see equations (8) and (9)).
- 4, A molecule occupies a single adsorption site and the orientation of the molecular axis corresponds to the IE minimum.
- 5, Molecular centre of gravity and molecular axis are fixed at the adsorption site.
- 6, Pairwise interactions with both the closest and second-order neighbours are included.
- 7, Possible interactions with the adsorbate molecules in the nearest cages are neglected.

Table 9. Lattice partition functions $q_{N_1 N_2}$ for different adsorbate configurations on zeolite $4A^a$ for adsorption sites relation 2:6 (N_i is the number of molecules on an adsorption site of type i).

N	N_1	N_2	$q_{N_1 N_2}$
0	0	0	1
1	1	0	2
	0	1	6
2	2	0	1
	1	1	$4x + 6y + 2$
	0	2	$7x + 6y + 2$
3	2	1	$2xy + 4x^2y$
	1	2	$10x^2y + 10xy + 4y + 4y^2 + 2y^3$
	0	3	$2y^3 + 8xy + 10x^2y$
4	2	2	$2x^4y^2 + 6x^3y^2 + 2x^3y^3 + 4x^2y^3 + x^2y^2$
	1	3	$2y^6 + 2x^4y^2 + 4x^3y^3 + 16x^3y^2 + 10x^2y^3 + 6x^2y^2$
	1	3	$2y^6 + 2x^4y^2 + 4x^3y^3 + 16x^3y^2 + 10x^2y^3 + 6x^2y^2$
	0	4	$5x^2y^2 + 6x^3y^2 + 2x^3y^3 + 2x^4y^2$
5	2	3	$2x^3y^5 + 8x^4y^4 + 10x^5y^4$
	1	4	$4x^3y^3 + 4x^4y^3 + 2x^3y^6 + 10x^4y^4 + 10x^5y^4$
	0	5	$2x^4y^3 + 4x^5y^4$
6	2	4	$8x^6y^6 + 7x^7y^6$
	1	5	$4x^7y^6 + 8x^6y^6$
	0	6	x^7y^6
7	2	5	$6x^9y^9$
	1	6	$2x^9y^9$
8	2	6	$x^{12}y^{12}$

^a $x = \exp(-w_1/kT)$, $y = \exp(-w_2/kT)$; values of w_1 , w_2 in figure 2.

The grand partition sum was expanded as [39]

$$\Xi = \sum_{N>0} Q_N \lambda^N, \quad (6)$$

where $\lambda = pA^3/kT$ is the absolute activity, $A = (2\pi MkT)^{-1/2}$, p is the pressure, M is the molecular mass, Q_N is the canonical partition function of an N molecule ensemble which has the following form for the approximation under discussion

$$Q_N = A^{-3N} \sum_{N_1, N_2} y_1^{N_1} y_2^{N_2} q_{N_1 N_2}, \quad (7)$$

where $y_I = j_I v_I^f \exp(-\epsilon_I/kT)$; N_I is the number of occupied AS of the I th type ($I = 1, 2$); $q_{N_1 N_2}$ is the lattice partition function for an N molecule configuration ($N = N_1 + N_2$); $q_{N_1 N_2} = \sum_{l, n} a_{ln} \exp(-nw_1/kT) \exp(-lw_2/kT)$; a_{ln} are the coefficients of lattice partition function calculated by us (see tables 9 and 10); w_1 , w_2 are interaction energies of molecules adsorbed at neighbouring sites (see figure 2); l , n are the numbers of w_1 and w_2 interactions, respectively, for an $(N_1 + N_2)$ configuration; j_I is the molecular partition function without translational degrees of freedom; and ϵ_I is the adsorption energy at the AS of the I th type,

$$\epsilon_I \cong E_I + \epsilon_{k|p', q'} + \frac{hcw_R^{(I)}}{2} - \begin{cases} 2B_X, & X = oH_2, pD_2 \\ 0, & X = pH_2, oD_2 \end{cases} \quad (8)$$

where $\epsilon_{k|p, q}$ is the energy of the rotational state; $p = (-1)^J$; $q = (-1)^m$; J and m are

Table 10. Lattice partition functions $q_{N_1 N_2}$ for different adsorbate configurations on zeolite $5A^a$ for adsorption sites relation 2:6 (N_i is the number of molecules on adsorption site of type i).

N	N_1	N_2	$q_{N_1 N_2}$
0	0	0	1
1	1	0	4
	0	1	4
2	2	0	6y
	1	1	4 + 12x
	0	2	6y
3	3	0	4y ³
	1	2	12y(x + x ²)
	2	1	12y(x + x ²)
	0	3	4y ³
4	4	0	y ⁶
	3	1	4y ³ (3x ² + x ³)
	2	2	24x ³ y ² + 6y ² (x ⁴ + x ²)
	1	3	4y ³ (3x ² + x ³)
	0	4	y ⁶
5	4	1	4x ³ y ⁶
	3	2	12y ⁴ (x ⁴ + x ⁵)
	2	3	12y ⁴ (x ⁴ + x ⁵)
	1	4	4x ³ y ⁶
6	4	2	6x ⁶ y ⁷
	3	3	4y ⁶ (x ⁶ + 3x ⁷)
	2	4	6x ⁶ y ⁷
7	4	3	4x ⁹ y ⁹
	3	4	4x ⁹ y ⁹
8	4	4	x ¹² y ¹²

^a $x = \exp(-w_1/kT)$, $y = \exp(-w_2/kT)$; values of w_1 , w_2 in figure 2.

the quantum numbers of angular rotational momentum and its projection in the coordinate frame of the AS of the I th type; k' , p' , q' are related to the lowermost rotational level of molecule X ((1, -1, -1) for X = oH₂, pD₂ and (1, 1, 1) for X = pH₂, oD₂); E_I is the interaction energy of the adsorbate at the I th type of AS with the zeolite lattice, $E_I = (E_{tot})_I$; B_X is the rotational constant of molecule X; and v_f^I is the free volume of adsorbate which, given the model approximations introduced above, is expressed, following reference [39], as

$$\begin{aligned}
 v_f^I &= \iiint \exp\left(-\frac{U(R, \theta, \Phi) - U(R_m, \theta_m, \Phi_m)}{kT}\right) d\tau \\
 &\cong \sum_{n_R} \exp\left(-\frac{E_{n_R}}{kT}\right) R_{n_R}^2 \int_{A_s} \int \exp\left(-\frac{U^{(n_R)}(\theta, \Phi) - U^{(n_R)}(\theta_m, \Phi_m)}{kT}\right) \sin \theta d\theta d\Phi
 \end{aligned}
 \tag{9}$$

where $d\tau = R^2 \sin \theta d\theta dR d\Phi$; $U^{(n_R)}(\theta, \Phi)$ is the profile of the IE over coordinates θ , Φ with fixed radial variable R_{n_R} at the n_R th vibrational state; $U^{(n_R)}(\theta_m, \Phi_m)$ is the minimum of the IE; E_{n_R} is the energy of the n_R th vibrational state; $E_{n_R} = hcw_R(n_R + 1/2)$; and A_s is the spherical angle of the AS.

The number of adsorbed molecules can be expressed via a partition function (equation (6)) as [39]

$$\bar{N} = \sum_{n>1} N Q_N \lambda^N / \sum_{N>0} Q_N \lambda^N. \quad (10)$$

Detailed discussion of computations of adsorption is beyond the scope of the present article and will be presented elsewhere [22].

Energetic inhomogeneity of zeolite 'surface', first mentioned in [3], might lead to nonuniform filling of sites which differ in adsorption energy and in local *o-p* separation coefficients. The models of 4A and 5A zeolites described above are used in the present work to estimate the average values of *o-p* separation coefficients for conditions which can be compared reasonably with the experimental data obtained for a limited range of temperatures and pressures.

For the discussed models of coverage of AS of two different kinds the average separation coefficients were determined by the equation

$$\bar{s} = \sum_N \lambda^N \sum_{N_1, N_2} s_{N_1, N_2} y_1^{N_1} y_2^{N_2} q_{N_1, N_2} / \sum_{N>0} Q_N \lambda^N \quad (11)$$

where s_{N_1, N_2} is the average *o-p* separation coefficient for the $(N_1 + N_2)$ configuration

$$s_{N_1, N_2} = (N_1 s_1 + N_2 s_2) / N, \quad (12)$$

where s_I is the *o-p* separation coefficient at AS of the I th kind. The values of s_I (indexes due to isotopic modifications are omitted for simplicity) were determined for the case of a single molecule adsorbed at the UC. Since for a coverage $\bar{N} < 8$ molecules per UC of the model lattice the values of \bar{s}_I vary insignificantly for simultaneous adsorption of molecules at neighbouring sites, these values can also be used for many-body cases. The negligible change in s_I is due to the slight influence of intermolecular interactions between molecules adsorbed on the model lattice on the total energy and barriers of hindered rotation (that can be seen easily from comparison of w_1 , w_2 and E_{tot} in figure 2).

Calculation of \bar{s}_I was accomplished assuming that rotation of the molecule axis, intramolecular vibration, and molecular translation can be separated; thus the molecular partition function can be reduced to a product $Q_r^{(i)} Q_v^{(i)} Q_t^{(i)}$, where $Q_r^{(i)} Q_v^{(i)} Q_t^{(i)}$ are the rotational, vibrational, and translational partition functions respectively in phase i ($i = \text{adsorbed (a) or gas (g)}$). For the model ignoring the interaction between the motions of the centre of mass of the molecule and the rotation of the axis, the *o-p* separation coefficients can be written as

$$(\bar{s}_{opX})_I = \frac{Q_{roX}^{(a)} Q_{rpX}^{(g)}}{Q_{rpX}^{(a)} Q_{roX}^{(g)}} \quad (13)$$

$$Q_{rj}^{(a)} = \sum_k \exp(-\epsilon_{k|p,q}/kT); \quad (14)$$

$$Q_{rj}^{(g)} = \sum_J (2J + 1) \exp\left(\frac{-BJ(J + 1)}{kT}\right). \quad (15)$$

6. Temperature dependence *o-p* separation coefficients for small coverage

Data on *o-p* separation coefficients obtained for small coverage [5] is more informative than that for high coverage, since the electrostatic fields of the ions are not screened by neighbouring molecules. This effect can be especially important for zeolite cavities with nearly spherical shapes. Moreover, another advantage of small coverage data is negligible adsorbate-adsorbate intermolecular interaction. It can be shown easily by comparing the zeolite-adsorbate interaction energies (IE) (the isosteric adsorption heat of equilibrium hydrogen on the 4A form is 7.96 kJ mol^{-1} [6]) with adsorbate-adsorbate IE (estimate for average IE of isolated pair $\text{H}_2\text{-H}_2$ is $-0.31 \text{ kJ mol}^{-1}$ [10]).

The temperature dependence of the *o-p* separation coefficients for small coverage for the model zeolite 4A presented in figure 8 shows that there is reasonable agreement between theory and experiment [5] within temperature range 135–160 K and for ionicity q_0 not exceeding 6.8. Generally, whatever factor might influence q_0 in different models, *o-p* separation coefficients would grow with the increase of q_0 due to the increasing interaction of the quadrupole moment of the adsorbate with the field of the ions. Thus, good agreement between theoretical and experimental data for small coverage of zeolite 4A is achieved. The consistent experimental data of two independent aspects—thermodynamic and spectroscopic—support the theoretical model of adsorbed molecules suggested in this article.

7. Comparison of *o-p* separation coefficients with experiment for medium coverage

The isobaric dependence of $\bar{s}_{op\text{H}_2}$ and $\bar{s}_{po\text{D}_2}$ calculated by us is given in figures 9 and 10, with chromatographic data [6, 7] measured at the equilibrium pressure, 1.4 atm, for which decrease of temperature results in increase of coverage of zeolite 4A (5A). In accordance with experiment [6], decrease of temperature from 98.9 K to

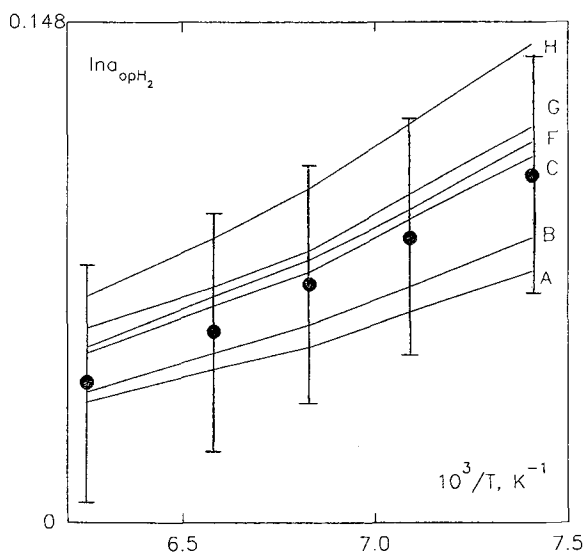


Figure 8. *Ortho-para* separation coefficients of H_2 for 4A zeolite for small coverage. The curves are in accordance with averaged dependence $\bar{s}_{op\text{H}_2}$ for the A, B, C, F, G, H models of the 4A zeolite. The experimental values [5] are shown by circles.

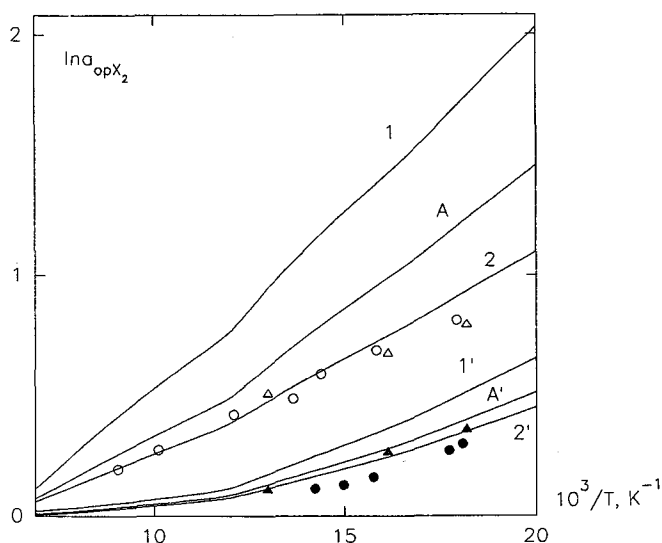


Figure 9. *Ortho-para* separation coefficients of H_2 and D_2 for zeolite 4A for medium coverage. Curves 1, 2 ($1'$, $2'$) show the dependence \bar{s}_{opH_2} (\bar{s}_{poD_2}) for the 1st and 2nd adsorption sites. Curves A (A') show the average dependence \bar{s}_{opH_2} (\bar{s}_{poD_2}) for the lattice from these types of centres (1st and 2nd). Experimental data are from Luk'janov [6] for H_2 (O) and D_2 (●); and from Leschev [7] for H_2 (Δ) and D_2 (\blacktriangle).

92.2 K leads to increase of coverage from 5.4 to 6.5 molecules per UC of zeolite 4A. The full range of application of the model from eight AS is limited by the region of coverage of about 5 or 6 molecules per UC [22] for the temperature interval noted before. The upper bound was shown by comparison of the calculated and experimental isotherms of the individual components [22]. The discrepancy between the

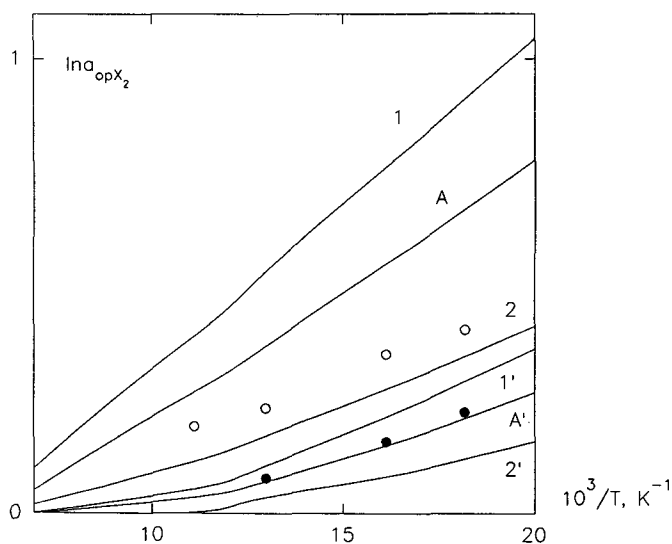


Figure 10. *Ortho-para* separation coefficients of H_2 , D_2 for zeolite 5A for medium coverage. Curves 1, 2 ($1'$, $2'$) show the dependence \bar{s}_{opH_2} (\bar{s}_{poD_2}) for the 1st and 2nd adsorption sites. Curves A (A') show the average dependence \bar{s}_{opH_2} (\bar{s}_{poD_2}) for the lattice from these types of sites (1st and 2nd). Experimental data are from Leschev [7] for H_2 (O) and D_2 (●).

theoretical (see average A dependence in figure 9) and experimental points s_{opH_2} for these and for higher coverages can be accounted for by the screening of the field of the Na_{III}^+ ion by the adjacent molecules.

The rotation barrier μ (equation (4)) in the plane which is parallel to one of the ring planes depends rigidly on the inhomogeneity of the field inside the unit cell. For higher coverage and with increased numbers of molecules adsorbed at the centres remote from the Na_{III}^+ ion, the value of μ for remote adsorption centres decreases, most likely due to the screening of the field of the Na_{III}^+ ion by adsorbed molecules. The decrease in μ results in the decrease of the computed values of the o - p separation coefficients. Similar deviation of the experimental points of \bar{s}_{pOD_2} from the theoretical results for zeolite 4A can be considered as a corroboration of the hypothesis.

Since, in agreement with this hypothesis, $\mu \rightarrow 0$ for saturation coverage, we have estimated the value of \bar{s}_{pOD_2} for high coverage (at $T = 25$ K) to compare it with the experimental value, $s_{pOD_2} = 3.41$ [40]. The computed value of 2.84 for $\mu = 0$ for centres of the 2nd type, which is the lower boundary of \bar{s}_{pOD_2} values, is in reasonable agreement with experiment.

The computations of IE have established that, in the case of zeolite 5A, the rotation barrier in the plane parallel to the lattice fragment can be taken to be zero for all of eight sites (due to the high symmetry of the positions of the cations: sodium and calcium cations form two different tetrahedra one of which is almost centrally symmetrical to the other, see figure 1(c)). Therefore, the effect of the adsorbed molecules on the nature of the adsorbate-adsorbent interaction energy is so small that the averages of \bar{s}_{opH_2} and \bar{s}_{pOD_2} stay within the range between the curves for the separate sites (see figure 10). Overestimation of theoretical values of \bar{s}_{opH_2} for zeolite 5A in comparison with the experimental values might be accounted for by the assumption of equality of q_0 for zeolites 4A and 5A. By lowering the ionicity of zeolite 5A below the q_0 of zeolite 4A we may decrease \bar{s}_{opH_2} and \bar{s}_{pOD_2} as in the case presented in figure 8.

The approach proposed provides the solution to the unresolved question on the higher selectivity of zeolite 4A over zeolite 5A in relation to the different o -, p -isomers. Comparison of the o - p H_2 , D_2 separation coefficients shows the essentially lower values on zeolite 5A compared with those on zeolite 4A. The anisotropic character of E_{el} on zeolite 4A (in the first row due to the interaction with the ion Na_{III}^+) leads to higher values of rotation barrier μ on all types of AS in relation to the similar AS of zeolite 5A (see table 7). As a consequence, the rotational level positions have a totally different structure on the zeolitic forms. The o - p H_2 , D_2 separation coefficients calculated in accordance with expressions (11) and (13) are more sensitive to small values of barrier μ , while barrier λ is greater on the AS of zeolite 5A (see table 7).

All results presented in this article are for the simplified zeolite model with two kinds of AS. The inclusion of the third sort of AS is especially necessary for medium and high coverage, where the zeolite-adsorbate interaction energy cannot be calculated correctly without taking into account the shielding by adsorbed molecules of the electrostatic field of the cations Na^+ . Moreover, such inclusion necessitates minimizing the total Gibbs energy of all adsorbed molecules as a result of the closeness of the zeolite-adsorbate and adsorbate-adsorbate energy interactions on the "expanded" lattice model. As a consequence, the much more complex adsorption model wholly different from the suggested simple lattice model must be used.

8. Conclusion

- (1) The new method for estimating adsorbent parameters (ionic charges) from the IR spectra of adsorbed molecules is proposed and implemented on model system zeolite A with diatomic molecules.
- (2) The zeolite parameters obtained let us compute in a self-consistent manner the spectroscopic and thermodynamic (ortho-para separation coefficients) values in good agreement with experimental data, for small coverage.
- (3) Analytical expressions for the lattice partition functions are suggested. Calculated in accordance with these, the *o-p* H₂ separation coefficients for model 4A zeolite with ionicity $q_0 < 6.8$ are in quantitative agreement with experimental values measured for small coverage.
- (4) Calculated *o-p* H₂, D₂ separation coefficients for model zeolites 4A and 5A are in reasonable qualitative agreement with experimental values measured for medium coverage. The explanation for higher *o-p* H₂, D₂ separation coefficients on zeolite 4A over those of zeolite 5A (owing to interaction with the ion Na_{III}⁺) is quantitatively supported.

The authors are very grateful to Dr L. R. Parbuzina for testing some results, and to Dr A. A. Luk'janov and Dr J. A. Leschev for permission to use unpublished data.

Appendix

The components of the total IE were calculated in accordance with expressions presented in reference [10, 13]

$$E_{\text{el}} = E_{\text{quad}} + E_{\text{hex}}$$

$$E_{\text{quad}} = -\frac{1}{4} \sum_i q_i (3 \cos^2 \nu_i - 1) \Theta_{zz} R_i^{-3} \quad (\text{A1})$$

$$E_{\text{hex}} = -\frac{1}{8} \sum_i q_i (35 \cos^4 \nu_i - 30 \cos^2 \nu_i + 3) \Phi_{zzzz} R_i^{-5}, \quad (\text{A2})$$

where q_i is the charge of ion i , ν_i is the angle between a molecular axis and a vector directed from molecular centre of gravity to ion i ; and Θ_{zz} and Φ_{zzzz} are components of the quadrupole and the hexadecapole electric moments, respectively.

$$E_{\text{ind}} = -\frac{1}{2} \sum_a (\alpha_{\parallel} T_a^2 \sin^2 \nu_a + a_{\perp} T_a^2 \cos^2 \nu_a) R_i^{-5} \quad (\text{A3})$$

where $T_a = \sum_i q_i (R_{ia} - R_{ma}) R_i^{-3}$; ν_a is the angle between a molecular axis and the coordinate a axis; R_{ia} is the a -component of vector R_i directed to ion i from the centre of a UC; R_{ma} is the a -component of vector R_m directed to the molecular centre of gravity from the centre of a UC.

$$E_{\text{disp}} + -\frac{1}{6} \sum_i (C_{\parallel}^i + 5C_{\perp}^i + 3(C_{\parallel}^i - C_{\perp}^i) \cos^2 \nu_i) R_i^{-6}, \quad (\text{A4})$$

where C_k^i are the dispersion constants for "ion-molecule" pairs in parallel ($k = \parallel$) or perpendicular ($k = \perp$) to the position of the molecular axis and the line connecting the molecular centre of gravity and ion i . Values C_k^i (hereafter expressed in Au) were estimated by the Kirkwood-Muller formula, equation (A5), which was successfully

used previously for similar calculations of the adsorption heats of inert gases on NaX [28]:

$$C_k^i = 6c^2 \frac{\alpha_k \alpha_i}{(\alpha_k/\chi_k) + (\alpha_i/\chi_i)}, \quad (\text{A5})$$

where α_i is the polarizability (Au) of ion i ,

$$\alpha_i = \frac{4}{9n} \left\{ \sum_{l=1}^n \langle r_l^2 \rangle \right\}^2, \quad (\text{A6})$$

where $\langle r_l^2 \rangle$ is the average square root radius of electron l in atom i ; α_k is the polarizability of a molecule in the k -orientation (see table 2); χ_k , χ_i are the diamagnetic susceptibilities (Au) of a molecule in the k -position and ion i , respectively, and were estimated by the Kirkwood relation

$$\chi_j = -\frac{1}{4c^2} \sqrt{(n\alpha_j)}, \quad (\text{A7})$$

where c is the velocity of light in a vacuum; n is the number of electrons in the atom; and $\alpha_j = (\alpha_i, \alpha_k)$.

$$E_{\text{rep}} = \sum_i (B_{\perp}^i \sin \nu_i + B_{\parallel}^i \cos \nu_i) R_i^{-12}, \quad (\text{A8})$$

where B_k^i are repulsive constants for "ion-molecule" pairs in parallel ($k = \parallel$) or perpendicular ($k = \perp$) positions to the molecular axis and the line connecting the molecular centre of gravity and an ion i .

The adsorbate-adsorbate ($a-b$) energy was taken as

$$E_{\text{im}} = E_{\text{im}}^{\text{disp}} + E_{\text{im}}^{\text{el}} + E_{\text{im}}^{\text{rep}}, \quad (\text{A9})$$

where expressions for the components E_{im}^q , $q = \text{disp, el, rep}$, (the sense of the indexes is the same as for the E_{tot} components) were as follows

$$E_{\text{im}}^{\text{disp}} = \sum_{l_a} \sum_{l_b} \Delta_{l_a l_b}^m(R) Y_{l_a}^{(m)}(\nu_a, \phi_a) Y_{l_b}^{(m)}(\nu_b, \phi_b), \quad (\text{A10})$$

where $\Delta_{00}^0 = -12.381 R^{-6}$, $\Delta_{20}^0 = -1.248 R^{-6}$, $\Delta_{22}^0 = -0.4004 R^{-6}$; R is the intermolecular distance; $Y_l^{(m)}$ are the spherical harmonics in the coordinate system with OZ axis directed along a line connecting the molecular centres of gravity

$$E_{\text{im}}^{\text{el}} = \frac{\Theta_{zz}^a \Theta_{zz}^b}{16R^5} (1 - 5(\cos^2 \nu_a + \cos^2 \nu_b) - 15 \cos^2 \nu_a \cos^2 \nu_b + 2(\sin \nu_a \sin \nu_b \cos(\phi_a - \phi_b) - 4 \cos \nu_a \cos \nu_b)^2), \quad (\text{A11})$$

where Θ_{zz}^a , Θ_{zz}^b are the quadrupole moment components of the interacting molecules $a-b$. The repulsive intermolecular energy was calculated in accordance with the De Bour expression [10] as

$$E_{\text{im}}^{\text{rep}} = 2.78 \sum_i \sum_j \exp(-1.78z_{ij}) \quad (\text{A12})$$

where z_{ij} is the internuclear separation.

References

- [1] OHKOSHI, S., FUJITA, Y., *et al.*, 1958, *Bull. chem. Soc. Jap.*, **31**, 770.
- [2] OHKOSHI, S., FUJITA, Y., *et al.*, 1958, *Bull. chem. Soc. Jap.*, **31**, 772.
- [3] BASMAJIAN, D., 1960, *Can. J. Chem.*, **38**, 141.
- [4] PARBUZIN, V. S., and PANCHENKOV, G. M., 1967, *Isotopenpraxis*, (3) **2**, 56.
- [5] GANT, P. L., YANG, K., *et al.*, 1970, *J. phys. Chem.*, **79**, 1985.
- [6] LUK'JANOV, A. A., 1989, Thesis, Moscow State University.
- [7] LESCHEV, J. A., 1989, Thesis, Moscow State University.
- [8] KOCHURIHIN, V. E., and ZEL'VENSII, J. D., 1969, *Zh. Fiz. Chim.*, **33**, 206.
- [9] PARBUZIN, V. S., and MALJAVSKII, N. I., 1975, *Dokl. Akad. Nauk SSSR*, **220**, 150.
- [10] HIRSCHFELDER, J. O., CURTIS, C. F., and BIRD, R. B., 1954, *Molecular Theory of Gases and Liquids* (Wiley).
- [11] LARIN, A. V., and PARBUZIN, V. S., 1987, *Russ. J. Phys. Chem.*, **61**, 866.
- [12] LARIN, A. V., and PARBUZIN, V. S., 1988, *Russ. J. Phys. Chem.*, **62**, 389.
- [13] PARBUZIN, V. S., and LARIN, A. V., 1988, *High-purity Substances*, **1**, 86.
- [14] FORSTER, H., and SCHULDT, M., 1978, *J. molec. Struct.*, **47**, 339.
- [15] FORSTER, H., and FREDE, W., 1984, *Infrared. Phys.*, **24**, 151.
- [16] COHEN DE LARA, E., 1989, *Molec. Phys.*, **66**, 477.
- [17] PLUTH, J. J., and SMITH, J. V., 1980, *J. Am. chem. Soc.*, **102**, 4704.
- [18] ZEFF, K., and SHOEMAKER, D. P., 1967, *Acta Crystallogr.*, **22**, 162.
- [19] DE BOOR, J. H., 1953, *The Dynamical Character of Adsorption* (Clarendon Press).
- [20] OZIN, G. A., BAKER, M. D., and GODBER, J., 1984, *J. chem. Phys.*, **88**, 4902.
- [21] FEDOROV, V. M., GLAZUN, B. A., *et al.*, 1964, *Izv. Akad. Nauk SSSR, Otd. chim. Nauk*, **11**, 1930.
- [22] LARIN, A. V., and PARBUZIN, V. S., unpublished.
- [23] LOPATKIN, A. A., 1983, *Theoretical Principles of Physical Adsorption* (MGU, Moscow).
- [24] TAKAISHI, T., and HOSOI, H., 1982, *J. phys. Chem.*, **86**, 2089.
- [25] KITTEL, C., 1975, *Introduction to Solid State Physics* (Wiley).
- [26] GORDON, A., and FORD, R., 1972, *Chemist's Companion* (Wiley).
- [27] BONDI, A., 1964, *J. chem. Phys.*, **68**, 441.
- [28] BROIER, P., KISELEV, A. V., *et al.*, 1968, *Zh. Fiz. Chim.*, **42**, 2556.
- [29] BARINSKII, R. L., and NEFEDOV, V. I., 1966, *X-Ray Spectral Determination of Atomic Charges in Molecules* (Nauka, Moscow).
- [30] BRATZEV, V. F., 1966, *Tables of Atomic Wave Functions* (Nauka, Moscow).
- [31] WOLNIEWICZ, L., 1966, *J. chem. Phys.*, **45**, 515.
- [32] HUNT, J. L., POLL, J. D., and WOLNIEWICZ, L., 1984, *Can. J. Phys.*, **62**, 1719.
- [33] POLL, J. D., and WOLNIEWICZ, L., 1978, *J. chem. Phys.*, **68**, 3053.
- [34] KOLOS, W., and WOLNIEWICZ, L., 1967, *J. chem. Phys.*, **46**, 1426.
- [35] AMOS, R. D., 1980, *Molec. Phys.*, **39**, 1.
- [36] EVETT, A. A., 1960, *J. chem. Phys.*, **33**, 789.
- [37] MACRURY, T. B., and SAMS, J. R., 1970, *Molec. Phys.*, **19**, 337.
- [38] COHEN DE LARA, E., and NGUEN TAN, T., 1976, *J. phys. Chem.*, **80**, 1917.
- [39] STEEL, W. A., 1967, *The Solid-Gas Interface*, Vol. 1 (Marcel Dekker).
- [40] ZHUN, G. G., private communication.
- [41] FARRAR, J. M., and LEE, V. T., 1972, *J. chem. Phys.*, **57**, 5492.
- [42] BUONTEMPO, U., CUNSOLO, S., *et al.*, 1966, *J. chem. Phys.*, **45**, 515.
- [43] BAKAEV, V. A., 1975, *Dokl. Akad. Nauk SSSR*, **221**, 861.